

Signals in single-event pion interferometry for granular sources of quark-gluon plasma dropletsWei-Ning Zhang,¹ Shu-Xia Li,¹ Cheuk-Yin Wong,^{2,3} and M. J. Efaaf¹¹*Department of Physics, Harbin Institute of Technology, Harbin, 150006, People's Republic of China*²*Physics Division, Oak Ridge National Laboratory, Oak Ridge, Tennessee 37831, USA*³*Department of Physics, University of Tennessee, Knoxville, Tennessee 37996, USA*

(Received 23 March 2005; published 30 June 2005)

We investigate two-pion Bose-Einstein correlations of quark-gluon plasma droplet sources in single-event measurements. We find that the distribution of the fluctuation between correlation functions of the single and mixed events provides useful signals to detect the granular structure of the source.

DOI: 10.1103/PhysRevC.71.064908

PACS number(s): 25.75.Nq, 25.75.Gz

I. INTRODUCTION

Recently, there has been much progress in the experimental search for the quark-gluon plasma [1,2]. Although there are many indications suggesting the presence of a very dense matter produced in high-energy heavy-ion collisions [1,2], a very important question is whether the produced dense matter is a quark-gluon plasma. If it is a quark-gluon plasma, it will undergo a phase transition from the quark-gluon plasma phase to the hadronic phase. It is desirable to search for the signature for the phase transition of the quark-gluon plasma.

The signature for the phase transition however depends sensitively on the order of the transition. Previously, it was suggested by Witten and many other workers that a granular structure of droplets occurs in a first-order QCD phase transition, and the observation of the granular structure can be used as a signature for a first-order QCD phase transition [3–15].

Recent lattice gauge calculations indicate that the phase transition at zero baryon chemical potential, $\mu_b = 0$, is likely to be a crossover transition. The transition becomes first order when μ_b is greater than a critical value μ_c [16–18]. Fodor and Katz found μ_c to be 360 MeV [17], although there may be uncertainties as the continuum extrapolation has not been carried out. Other theoretical estimates of Ejiri *et al.* give a value of μ_c from 52 to 140 MeV [16]. Clearly, whatever the theoretical predictions may be, it is ultimately an experimental question to explore the order of the phase transition empirically. Because the baryon density increases as the rapidity increases, the variation of the phase transition order as a function of rapidity will provide additional information on the location of the critical point μ_c .

Recent Hanbury-Brown-Twiss (HBT) intensity interferometry measurements indicate that $R_{\text{out}}/R_{\text{side}} \sim 1$, whereas the traditional hydrodynamical model predicts a much larger ratio [19–21]. Previous descriptions of these HBT radii were presented in terms of the hadronic cascade model of Humanic [22], the parton cascade model of Lin *et al.* [23] and Molnár and Gyulassy [24], and the hydrodynamical Buda-Lund model of Csanád *et al.* [25]. The puzzling aspect of the HBT measurement may also arise from other considerations. In a recent analysis, a granular emitting source of droplets was put forth to explain the HBT puzzle for nucleus-nucleus collisions at Brookhaven National Laboratory's Relativistic

Heavy Ion Collider (RHIC) [14]. The suggestion was based on the observation that, in the hydrodynamical model [19,20], the particle emission time scales with the radius of the droplet. Particles will be emitted earlier if the radius of the droplet is smaller, as in a source of many droplets. An earlier emission time will lead to a smaller extracted HBT radius R_{out} . As a result, the value of R_{out} can be close to R_{side} for a granular quark-gluon plasma source [14].

Previously, Pratt *et al.* studied the HBT interferometry of granular droplets by averaging over many events [6]. Methods to detect a granular structure by the single-event intensity interferometry were recently proposed [26]. It was found that the single-event correlation function from a chaotic source of granular droplets exhibits large fluctuations, with maxima and minima at relative momenta that depend on the relative coordinates of the droplet centers. The presence of this type of maxima and minima of a single-event correlation function at many relative momenta is a signature for a granular structure and a first-order QCD phase transition [26].

The difficulty of using the single-event two-pion interferometry at RHIC arises because of the small number of pion pairs with small relative momenta. In a typical single event of a nearly head-on collision at very high energies at RHIC, the number of identical pions is of the order of a few thousand. The number of observed identical pions n_π is only a small fraction of this number. For example, the number of identical pions detected in the STAR Collaboration in the most central Au + Au collisions at RHIC is of the order of a few hundred [27]. Although the number of pairs of identical pions in the event varies as $N_{\pi\pi} = n_\pi(n_\pi - 1)/2$, only a small fraction of these pairs have relative momentum small enough to be useful in a HBT analysis. The number of pion pairs in each relative momentum bin may be so small that there can be large associated statistical errors.

Instead of trying to obtain the detailed granular structure of the emitting source in each event at present, it will be useful in the initial stage to have a more modest goal. It is desirable to see whether the correlation functions indicate possible signals for a granular structure. More refined study of the granular structure can follow after the initial stage becomes successful.

Accordingly, we shall try to outline a method to extract the signals for the granular structure. Our idea is to calculate the fluctuations of the single event correlation function relative to its corresponding mixed-event correlation function. The

difference constitutes the “signal” for the event in question. The distribution of these fluctuations (in units of their statistical errors), collected for a large number of single events to enhance statistics, would have a wider distribution for a granular structure, compared to those from an emitting source without the granular structure. The distribution of the correlation function fluctuations provides a useful tool to detect the granular structure of the source. In particular, the root-mean-square fluctuation, in the case of a granular droplet structure, increases when the number of droplets decreases. If the phase transition is accompanied by only a few droplets, the signal may be large enough to make it detectable. In what follows, we would like to analyze whether this method may be feasible.

II. SINGLE-EVENT AND MIXED-EVENT TWO-PION CORRELATION FUNCTIONS

The two-particle Bose-Einstein correlation function for the detection of identical pions with momenta k_1 and k_2 is defined as $C(k_1, k_2) = P(k_1, k_2)/P(k_1)P(k_2)$, where $P(k_1, k_2)$ is the two-particle momentum distribution, $P(k_i)$ is the single-particle momentum distribution with momentum k_i , and the momenta are measured in the source center-of-mass frame. For a chaotic pion-emitting source, $P(k_i)$ ($i = 1, 2$) is

$$P(k_i) = \sum_{X_i} A^2(k_i, X_i), \quad (1)$$

where $A(k_i, X_i)$ is the magnitude of the amplitude for emitting a pion with 4-momentum $k_i = (E_i, \mathbf{k}_i)$ at X_i . The two-particle distribution function $P(k_1, k_2)$ can be expressed as

$$P(k_1, k_2) = \sum_{X_1, X_2} |\Phi(k_1, k_2; X_1, X_2)|^2, \quad (2)$$

where $\Phi(k_1, k_2; X_1, X_2)$ is the two-pion wave function. Neglecting the absorption of the emitted pions by other droplets, we write $\Phi(k_1, k_2; X_1, X_2)$ simply [28] as

$$\begin{aligned} \Phi(k_1, k_2; X_1, X_2) &= \frac{1}{\sqrt{2}} [A(k_1, X_1)A(k_2, X_2)e^{ik_1 \cdot X_1 + ik_2 \cdot X_2} \\ &\quad + A(k_1, X_2)A(k_2, X_1)e^{ik_1 \cdot X_2 + ik_2 \cdot X_1}]. \end{aligned} \quad (3)$$

The correlation function $C(k_1, k_2)$ is in general a function of the 4-dimensional momenta $k_1 - k_2$ and $k_1 + k_2$. Previous results of the single-event correlation function of granular droplets indicate large fluctuations as a function of the relative 4-momentum $k_1 - k_2$, having maxima and minima at locations that depend on the relative coordinates of the droplet centers [26]. To map out the details of such a multidimensional correlation function, it is necessary to have a large number of pion pairs in a single event, which may be beyond the capabilities of present detectors and accelerators. With limited statistics as would likely be the case, we can first study the simplifying case by concentrating on a small number of degrees of freedom and integrating out other degrees of freedom so that the statistical errors in the correlation function can be smaller. For this purpose, we shall study the correlation function as a function of the variable $q = |\mathbf{k}_1 - \mathbf{k}_2|$ in the

source center-of-mass frame for which the other degrees of freedom have been integrated out.

In our numerical work for a granular source with N_d droplets, we obtain the single-event and mixed-event two-pion correlation functions for the granular source with the following steps:

Step 1: Generate the space-time coordinates R_j ($j = 1, 2, \dots, N_d$) of the droplet centers according to a distribution of the droplet centers.

Step 2: Select the two emitting pions from the droplets randomly, and get the space-time coordinates X_1 and X_2 of the pions in the source center-of-mass frame according to the density distribution of the droplets, the coordinates of the droplet centers, and the collective velocities at the emission points, $\mathbf{v}(X_i)$ ($i = 1, 2$).

Step 3: Generate the momenta $k'_1 = (E'_1, \mathbf{k}'_1)$ and $k'_2 = (E'_2, \mathbf{k}'_2)$ of the two pions in the frame in which the source element is at rest according to the distribution $A^2(k'_i, X)$, taken to be the Bose-Einstein distribution characterized by the temperature T_f , and obtain their momenta k_1 and k_2 in the source center-of-mass frame by Lorentz transformation if the source element is boosted in the source center-of-mass frame.

Step 4: Accumulate the event in the bin of the corresponding relative momentum variable $q = |\mathbf{k}_1 - \mathbf{k}_2|$ with the weight factor w_{11} for the probability $P(k_1)P(k_2)$ for a pair of uncorrelated pions of relative momentum q , and with the weight factor w_{12} for the probability $P(k_1, k_2)$ for a pair of correlated pions of relative momentum q ,

$$w_{11} = [E'_1/E_1][E'_2/E_2], \quad (4)$$

$$\begin{aligned} w_{12} &= \frac{1}{2} \left| \sqrt{E'_1/E_1} \sqrt{E'_2/E_2} e^{ik_1 \cdot X_1 + ik_2 \cdot X_2} \right. \\ &\quad \left. + \sqrt{E'_{12}/E_1} \sqrt{E'_{21}/E_2} e^{ik_1 \cdot X_2 + ik_2 \cdot X_1} \right|^2, \end{aligned} \quad (5)$$

where E'_{ij} ($i, j = 1, 2$) is the energy of the i th pion in the frame in which the source element at X_j is at rest, which is obtained from E_i by a reverse Lorentz transformation with the collective velocity $\mathbf{v}(X_j)$.

Step 5: Repeat steps 2 through 4 for $N_{\pi\pi}$ pairs of pions in a single event. We label the distributions obtained for $P(k_1)P(k_2)$ for a pair of uncorrelated pions by $\text{Uncor}_s(q)$ and the distribution of $P(k_1, k_2)$ for a pair of correlated pions by $\text{Cor}_s(q)$.

Step 6: Repeat steps 1 through 5 for N_{event} number of different events, and obtain the mixed-event correlated and uncorrelated pion-pair distributions $\text{Cor}_m(q)$ and $\text{Uncor}_m(q)$, by summing $\text{Cor}_s(q)$ and $\text{Uncor}_s(q)$ of the N_{event} different events.

Step 7: Obtain the single-event correlation function $C_s(q)$ by dividing $\text{Cor}_s(q)$ by $\text{Uncor}_m(q)$ and the mixed-event correlation function $C_m(q)$ by dividing $\text{Cor}_m(q)$ by $\text{Uncor}_m(q)$.

We first investigate the two-pion correlation functions for N_d static granular droplet sources. The centers of the droplets are assumed to follow a Gaussian distribution with a standard deviation σ_R , and the density distribution of each droplet is assumed to be given by a Gaussian distribution with a standard deviation σ_d . In our numerical examples,

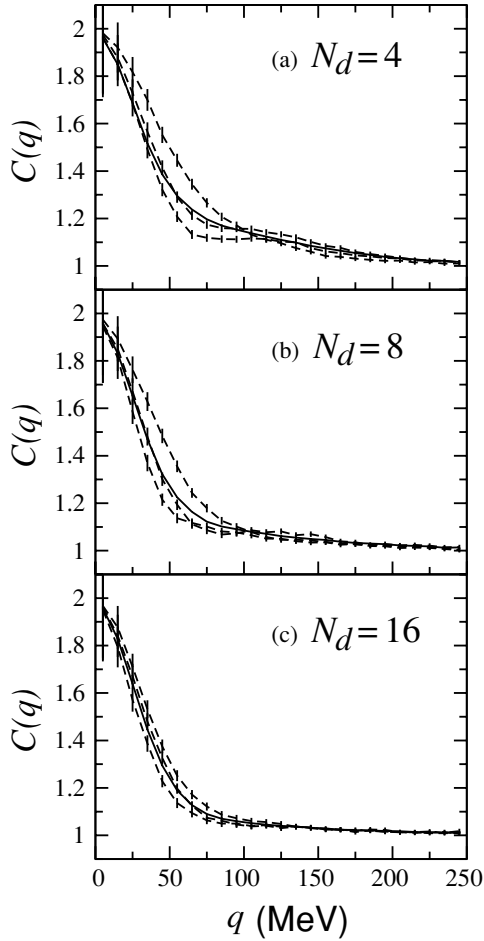


FIG. 1. Two-pion correlation functions for a sample of different single events (dashed lines) and mixed events (solid lines) for static granular sources of N_d droplets.

σ_R and σ_d are taken as 5.0 and 1.5 fm, respectively, and the thermal emission temperature of the pions is taken to be $0.65T_c = 0.65 \times 160 = 104$ MeV. Figures 1(a)–1(c) show the two-pion correlation functions for the granular sources with $N_d = 4, 8,$ and 16 , respectively. In each figure the dashed lines give the correlation function $C(q)$ for a sample of different single events, each of which has a correlated pion-pair distribution $\text{Cor}_s(q)$ calculated with $N_{\pi\pi} = 10^6$ pion pairs within $q \leq 250$ MeV, and the solid line is for the mixed-event obtained by averaging $N_{\text{event}} = 10^3$ single events. One can see that there are fluctuations for the single-event correlation functions relative to the mixed-event correlation function, and the fluctuations increase as N_d decreases.

III. DISTRIBUTION OF THE FLUCTUATION OF SINGLE-EVENT TWO-PION CORRELATION FUNCTION

From the results in Fig. 1, we observe that the correlation function $C_s(q)$ for individual single events fluctuates with respect to the mixed-event correlation function $C_m(q)$. We can make the fluctuation quantitative and introduce the fluctuation

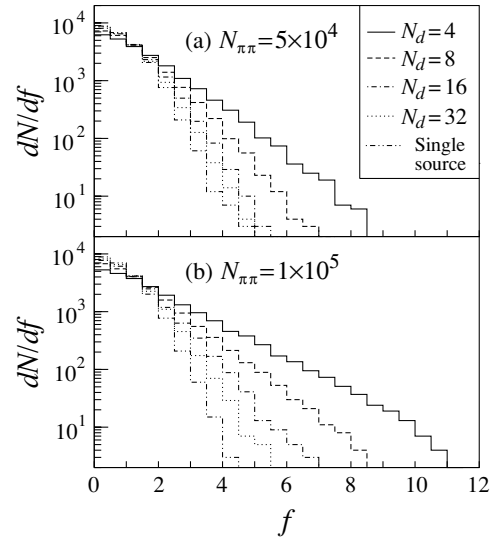


FIG. 2. The distributions dN/df of f for (a) $N_{\pi\pi} = 5 \times 10^4$ and (b) $N_{\pi\pi} = 10^5$.

as the difference between the single-event correlation function and the mixed-event correlation function. To take into account the error of the measurement, we weigh the fluctuation by the inverse of the corresponding error and define the fluctuation quantitatively as

$$f(q) = \frac{|C_s(q) - C_m(q)|}{\Delta|C_s(q) - C_m(q)|}, \quad (6)$$

where $\Delta|C_s(q) - C_m(q)|$ is the error in the measurement of $C_s(q) - C_m(q)$ given by

$$\begin{aligned} \Delta|C_s(q) - C_m(q)| &= \Delta C_s(q) + \Delta C_m(q) \simeq \Delta C_s(q) \\ &\simeq C_s(q) \left\{ \frac{1}{\sqrt{N_{\pi\pi}}} + \frac{1}{\sqrt{\text{Cor}_s(q)}} \right\}. \end{aligned} \quad (7)$$

We calculate the distribution of the fluctuation f for the sources with different numbers of droplets. In these calculations, we take the width of the relative momentum bin as 10 MeV and use the bins in the region $20 \leq q \leq 250$ MeV. Figures 2(a) and 2(b) show the distributions of f for $N_d = 4, 8, 16,$ and 32 , obtained from 1000 single events, each of which has the correlated pion-pair distribution $\text{Cor}_s(q)$ calculated with $N_{\pi\pi} = 5 \times 10^4$ and 10^5 pion pairs within $q \leq 250$ MeV. The standard deviations σ_R and σ_d for the granular sources are 5.0 and 1.5 fm, respectively. The results for a nongranular single source with a Gaussian density distribution with 5.0 fm standard deviation are also shown as a reference. It can be seen that the distributions for the granular sources are wider than that for the single source. The width of the distribution for the granular source decreases with N_d .

From the distribution of f , one can calculate the root-mean-square values of f . Figures 3(a) and 3(b) show the root-mean-square f as a function of N_d for sources with $\sigma_R = 5.0$ and 7.0 fm obtained for the cases of $N_{\pi\pi} = 10^5$ and $\sigma_d = 1.5$ fm and of $N_{\pi\pi} = 5 \times 10^4$ and $\sigma_d = 2.0, 1.5,$ and 1.0 fm. The double-dot-dashed lines are the root-mean-square

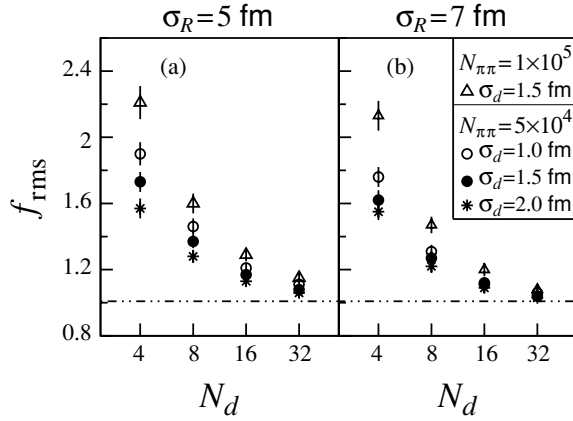


FIG. 3. The root-mean-square f as a function of N_d for static granular sources. The double-dot-dashed lines are the result for a single Gaussian source.

f for the distribution of the single Gaussian source in Fig. 2. It can be seen that f_{rms} is sensitive to N_d and decreases as σ_d and σ_R increase. With the values of f_{rms} , one may distinguish the granular source with $N_d = 16$ from the single Gaussian source with $N_{\pi\pi} = 5 \times 10^4$ pairs of identical pions, and one may even distinguish the granular sources up to $N_d = 32$ with $N_{\pi\pi} = 10^5$ identical pions.

IV. DISTRIBUTION OF THE FLUCTUATION FOR HYDRODYNAMICAL QUARK-GLUON PLASMA DROPLET SOURCE

We investigate next the distribution of f for a granular sources of quark-gluon plasma droplets that evolve hydrodynamically. We assume that all of the droplets in the source have the same initial radius $r_d = 1.5$ fm and evolve hydrodynamically in the same way. We use relativistic hydrodynamics with the equation of state of the entropy density [29,30] to describe the evolution of the droplets [14,19,20], and we take the temperature width of the transition as $\Delta T = 0.05$ and the initial conditions of the droplets as [14,19,20]

$$\begin{aligned} \epsilon'(t' = 0, r') &= \begin{cases} \epsilon_0, & r' < r_d, \\ 0, & r' > r_d, \end{cases} \\ v'(t' = 0, r') &= 0, \end{aligned} \quad (8)$$

where r' , ϵ' , and v' are, respectively, the radial coordinate, energy density, and velocity of a fluid element in the droplet rest frame, and $\epsilon_0 = 1.875T_c s_c$ [19,20] is the initial energy density of the droplets. The initial distribution of the droplet centers is taken to be a Gaussian distribution with the standard deviation $\sigma_R = 5.0$ fm. For the case with an additional collective radial expansion, the droplet centers are assumed to have a constant radial velocity v_d in the center-of-mass frame of the granular source [14]. To reduce the influence of source lifetime on our observations for the granular structure [6], we use the “side” component of the relative momentum of the two pions, q_s (perpendicular to the total momentum of the two pions), as the variable [31–34] for the

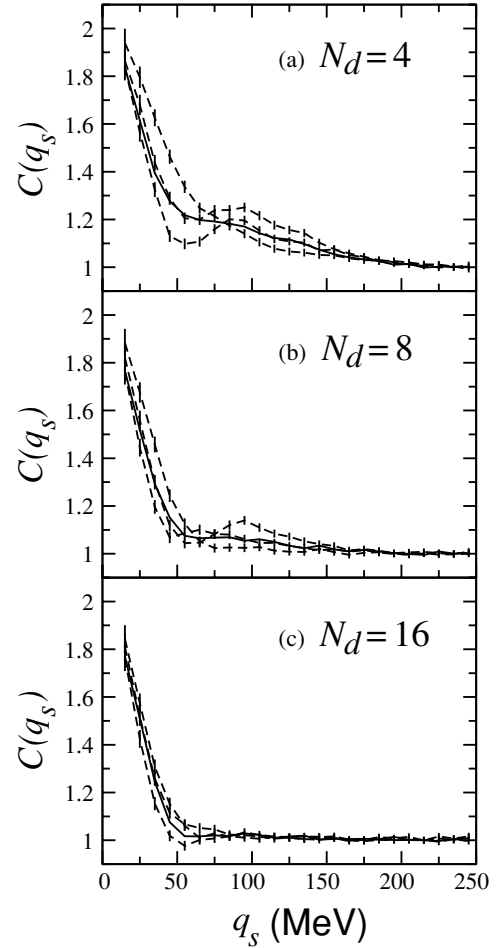


FIG. 4. Two-pion correlation functions for a sample of different single events (dashed lines) and mixed events (solid lines) of the dynamical granular sources.

granular source of hydrodynamic-evolution quark-gluon plasma droplets. Figures 4(a)–4(c) show the correlation function $C(q_s)$ (with $q_{\text{out}} \leq 20$ MeV) for the dynamical granular sources with $v_d = 0.5$ and $N_d = 4, 8,$ and 16 , respectively. In each figure the dashed lines give the correlation function $C(q_s)$ for a sample of different single events, each of which has a correlated pion-pair distribution $\text{Cor}_s(q_s)$ calculated with $N_{\pi\pi} = 10^6$ pion pairs within $q_s \leq 250$ MeV, and the solid line is for the mixed-event obtained by averaging $N_{\text{event}} = 10^3$ single events. The freeze-out temperature of the pions is taken to be $0.65T_c = 0.65 \times 160 = 104$ MeV.

Figures 5(a) and 5(b) show the distributions of f for the dynamic granular sources with $v_d = 0$ and $v_d = 0.5$, and $N_d = 4, 8, 16,$ and 32 . The double-dot-dashed lines are for a dynamical single source with initial radius $r_d = 5.0$ fm as a reference. The number of pion pairs within $q_s \leq 250$ MeV for one single event is $N_{\pi\pi} = 5 \times 10^4$ and the number of events is $N_{\text{event}} = 10^3$ for all the distributions. Because of the hydrodynamical evolution of the droplet, the single-droplet source has a collective radial expansion. However, the multidroplet granular source does not have a collective radial expansion when $v_d = 0$. When $v_d \neq 0$ the width of the

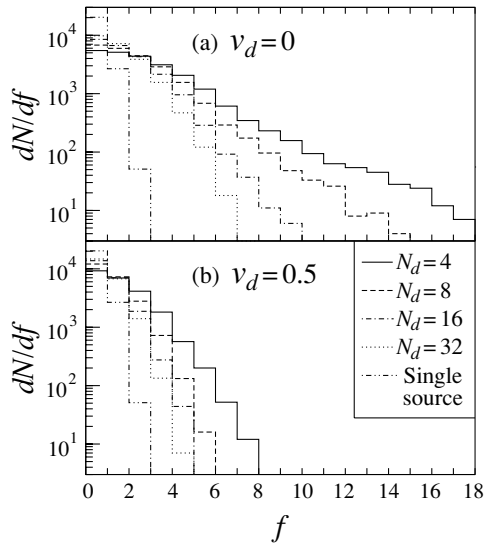


FIG. 5. The distributions of f for the dynamical quark-gluon plasma granular sources with $v_d = 0$ and 0.5 .

distributions for the granular sources decreases because of the additional collective radial expansion velocity v_d .

Figures 6(a) and 6(b) show the root-mean-square values of f calculated from the distributions of 1000 single events for the dynamical granular sources with $v_d = 0$ and 0.5 , respectively. The Δ symbols are for the case of the number $N_{\pi\pi}$ of the pion pair within $q_s \leq 250$ MeV for one single event is 10^5 . The \bullet and $*$ symbols are for the cases of $N_{\pi\pi} = 5 \times 10^4$ with and without the constraint $q_o \leq 20$ MeV. The double-dot-dashed lines are the result for the distribution of the single-droplet source in Fig. 5. One observes that f_{rms} for the granular sources are larger than that for the single-droplet source, and the root-mean-square f for the granular sources increase with $N_{\pi\pi}$. Although the f_{rms} results with the constraint $q_o \leq 20$ MeV are larger than those without the constraint, our simulations indicate that this constraint is very restrictive and only about 3.5% of the pion pairs within $q_s \leq 250$ MeV satisfy it. As the droplet number decreases, the fluctuation increases. The effect of the increase becomes less pronounced as the collective expansion velocity increases.

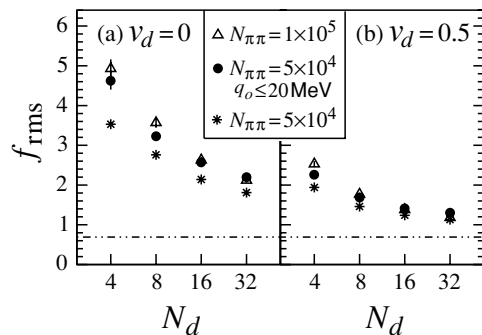


FIG. 6. The root-mean-square f as a function of N_d for dynamical granular sources.

V. CONCLUSIONS AND DISCUSSION

Recent experiments at RHIC provide ample evidence for a dense matter produced in high-energy heavy-ion collisions. Is the produced dense matter the quark-gluon plasma? If so, what is the order of its phase transition? Because a granular structure of droplets occurs in a first-order QCD phase transition, the observation of the granular structure can be used as a signature for a first-order QCD phase transition [3–15].

We would like to develop tools to use HBT interferometry to examine the granular droplet structure of the dense matter if it is produced in high-energy heavy-ion collisions. We showed previously that the single-event correlation function in HBT interferometry for granular droplets exhibits oscillations, depending on the relative coordinates of the droplet centers [26]. In realistic experimental situations, the number of identical pion pairs in each single event is limited. We continue our investigation here to find appropriate measurable quantities that could be used to detect granular structure in HBT measurements.

In our present investigation, we study the fluctuation between the single-event correlation function and the mixed-event correlation function and find that the distribution of the correlation function fluctuation f between the single-event and the mixed-event correlation functions can be a measurable quantity that could be used to probe the granular droplet structure. The width of the distribution is greater for a granular source than for a single source, and the width increases as the droplet number decreases. The effect of the increase becomes less pronounced when the droplets have a collective expansion. These changes of widths can be quantified in terms of the root-mean-square fluctuation of f . The f_{rms} for a granular droplet source increases with the number of identical pion pairs in an event. The detection of the granular droplets becomes more favorable as the number of identical pairs increases.

Our numerical simulated calculations indicate that the correlation function fluctuation leads to detectable differences if the droplet number is small (less than or equal to 16) and the number of identical pairs in each single event is of order 5×10^4 or more. At RHIC energies, the multiplicity of an identical pion event is about a few hundred, and the number of pion pairs in an event is about 10^5 . In this case, it may be possible to reveal the source granularity by the distribution f constructed with 1000 events with almost the same identical pion multiplicity (same impact parameter) if $N_d \leq 16$. One can infer from Fig. 6(b) that in the measurement of f_{rms} a precision of 1.3 units will allow one to test or exclude the hypothesis of a granular source of 4 droplets, a precision of 0.9 units will allow one to test or exclude 8 droplets, and a precision of 0.6 units will allow one to test or exclude 16 droplets. So, it will be of interest to see whether the correlation function fluctuation can indeed be measured at RHIC. The situation becomes even more favorable for Large Hadron Collider collisions at higher energies, where there can be a greater number of identical pion pairs.

As with the development of many new experimental tools, progress is made by gradually increasing the complexity of one's scope of research and the areas of focus. In the present analysis, we have not considered the absorption and

the multiple scattering of the pions [35,36]. Investigations on these effects can be carried out in the future to see how they may modify the distribution of the fluctuations. We have also not considered the fluctuation of the overall size of the emission source, which clearly depends on the experimental selection and will require an investigation in conjunction with the experimental setup and selections. An event multiplicity cut may be needed to reduce the fluctuation resulting from the sizes of the emitting source. Future investigations to refine the tool of HBT measurements for the detection of granular

structure will be of great interest to probe the order of the quark-gluon plasma phase transition.

ACKNOWLEDGMENTS

This research was supported by the National Natural Science Foundation of China under Contract No. 10275015 and by the Division of Nuclear Physics, US DOE, under Contract No. DE-AC05-00OR22725 managed by UT-Battle, LC.

-
- [1] M. Gyulassy and L. McLerran, Nucl. Phys. **A750**, 30 (2005).
 [2] See also *New Discoveries at RHIC: The Current Case for the Strongly Interactive QGP*, RIKEN Scientific Articles, Vol. 9, BNL, May 14–15, 2004 published as Nuclear Physics A, Vol. 750, 2005.
 [3] E. Witten, Phys. Rev. D **30**, 272 (1984).
 [4] D. Seibert, Phys. Rev. Lett. **63**, 136 (1989).
 [5] T. Kajino, Phys. Rev. Lett. **66**, 125 (1991).
 [6] S. Pratt, P. J. Siemens, and A. P. Vischer, Phys. Rev. Lett. **68**, 1109 (1992).
 [7] L. P. Csernai and J. I. Kapusta, Phys. Rev. D **46**, 1379 (1992); L. P. Csernai and J. I. Kapusta, Phys. Rev. Lett. **69**, 737 (1992).
 [8] R. Venugopalan and A. P. Vischer, Phys. Rev. E **49**, 5849 (1994).
 [9] W. N. Zhang, Y. M. Liu, L. Huo, Y. Z. Jiang, D. Keane, and S. Y. Fung, Phys. Rev. C **51**, 922 (1995).
 [10] S. Alamoudi, D. G. Barci, D. Boyanovsky, C. A. A. deCarvalho, E. S. Fraga, S. E. Joras, and F. I. Takakura, Phys. Rev. D **60**, 125003 (1999).
 [11] W. N. Zhang, G. X. Tang, X. J. Chen, L. Huo, Y. M. Liu, and S. Zhang, Phys. Rev. C **62**, 044903 (2000).
 [12] L. P. Csernai, J. I. Kapusta, and E. Osnes, Phys. Rev. D **67**, 045003 (2003).
 [13] J. Randrup, Phys. Rev. Lett. **92**, 122301 (2004).
 [14] W. N. Zhang, M. J. Efaaf, and C. Y. Wong, Phys. Rev. C **70**, 024903 (2004).
 [15] J. Randrup, nucl-th/0406031.
 [16] S. Ejiri, C. R. Allton, S. J. Hands, O. Kaczmarek, F. Karsch, E. Laermann, and C. Schmidt, Prog. Theor. Phys. Suppl. **153**, 118 (2004).
 [17] Z. Fodor and S. D. Katz, J. High Energy Phys. **04** (2004) 050.
 [18] K. Redlich, F. Karsch, and A. Tawfik, J. Phys. G **30**, S1271 (2004).
 [19] D. H. Rischke and M. Gyulassy, Nucl. Phys. **A608**, 479 (1996).
 [20] D. H. Rischke, in Proceedings of the 11th Chris Engelbrecht Summer School in Theoretical Physics, (Cape Town, February 1998), nucl-th/9809044.
 [21] U. Heinz and P. Kolb, Nucl. Phys. **A702**, 269 (2002).
 [22] T. Humanic, Nucl. Phys. **A715**, 641 (2003).
 [23] Z. W. Lin, C. M. Ko, and S. Pal, Phys. Rev. Lett. **89**, 152301 (2002).
 [24] D. Molnár and M. Gyulassy, Heavy Ion Phys. **18**, 69 (2003); D. Molnár and M. Gyulassy, Phys. Rev. Lett. **92**, 052301 (2004).
 [25] M. Csanád, T. Csörgó, B. Lörstad, and A. Ster, J. Phys. G **30**, S1079 (2004); M. Csanád, T. Csörgó, B. Lörstad, and A. Ster, Acta Phys. Pol. B **35**, 191 (2004); M. Csanád, T. Csörgó, B. Lörstad, and A. Ster, Nukleonika **49**, S49 (2004), nucl-th/0402037.
 [26] C. Y. Wong and W. N. Zhang, Phys. Rev. C **70**, 064904 (2004).
 [27] J. Adams *et al.* (STAR Collaboration), submitted to Phys. Rev. C (nucl-ex/0311017).
 [28] C. Y. Wong, *Introduction to High-Energy Heavy-Ion Collisions* (World Scientific, Singapore, 1994), Chap. 17.
 [29] J. P. Blaizot and J. Y. Ollitrault, Phys. Rev. D **36**, 916 (1987).
 [30] E. Laermann, Nucl. Phys. **A610**, 1 (1996).
 [31] S. Pratt, Phys. Rev. Lett. **53**, 1219 (1984); S. Pratt, Phys. Rev. D **33**, 72 (1986); S. Pratt, T. Csörgó, and J. Zimányi, Phys. Rev. C **42**, 2646 (1990).
 [32] G. Bertsch, M. Gong, and M. Tohyama, Phys. Rev. C **37**, 1896 (1988); G. Bertsch, Nucl. Phys. **A498**, 173c (1989).
 [33] U. A. Wiedemann and U. Heinz, Phys. Rep. **319**, 145 (1999).
 [34] R. M. Weiner, Phys. Rep. **327**, 249 (2002).
 [35] C. Y. Wong, J. Phys. G **29**, 2151 (2003); C. Y. Wong, J. Phys. G **30**, S1053 (2004).
 [36] W. N. Zhang, M. J. Efaaf, C. Y. Wong, and M. Khaliliasr, Chin. Phys. Lett. **21**, 1918 (2004).